International Journal of Earth, Energy and Environmental Sciences
ISSN: 2517-942X
Vol:13, No:4, 2019

# Evaluating Hurst Parameters and Fractal Dimensions of Surveyed Dataset of Tailings Dam Embankment

I. Yakubu, Y. Y. Ziggah, C. Yeboah

***Abstract*****—**In the mining environment, tailings dam embankment is among the hazards and risk areas. The tailings dam embankment could fail and result to damages to facilities, human injuries or even fatalities. Periodic monitoring of the dam embankment is needed to help assess the safety of the tailings dam embankment. Artificial intelligence techniques such as fractals can be used to analyse the stability of the monitored dataset from survey measurement techniques. In this paper, the fractal dimension (D) was determined using D = 2-H. The Hurst parameters (H) of each monitored prism were determined by using a time domain of rescaled range programming in MATLAB software. The fractal dimensions of each monitored prism were determined based on the values of H. The results reveal that the values of the determined H were all within the threshold of $0 \leq H \leq 1$ m. The smaller the H, the bigger the fractal dimension is. Fractal dimension values ranging from $1.359 \times 10^{-4}$ m to $1.8843 \times 10^{-3}$ m were obtained from the monitored prisms on the based on the tailing dam embankment dataset used. The ranges of values obtained indicate that the tailings dam embankment is stable.

***Keywords*****—**Hurst parameter, fractal dimension, tailings dam embankment, surveyed dataset.

## I. Introduction

TAILINGS, also called mine dumps or leach residues are the materials left over after the process of separating the valuable part from the gangue of an ore [1]. Tailings are different from overburden. Overburden represents gangue or other material that lies on top of an ore and is removed in the process of mining and remains untreated [2]. Dams are usually constructed to store the tailings. A tailings dam is typically an earth-filled embankment dam used to stockpile by-products of mining operations after separating the ore from the gangue [3]. Tailings dams are some of the major man-made structures on earth. One of the most technically challenging areas for geotechnical engineers is how to maintain and monitor tailings dams. Over the last few decades, many tailings dam failures have occurred, and it is projected that about two to five major failures occur per year [4], [5]. Instability and likelihood of dam failure has a larger impact on the safety of mine workers and built-up infrastructure with concomitant environmental effects. Tailings dam collapse in mines are on the rise [6]. The safety of these tailings dams has therefore become a major concern globally. Historical dam failure reveals three major causes: (i) leaching and internal erosion in the embankment (ii) leaching and erosion of the base and (iii) erosion of the overtopping [7].

Tailings dam embankment saturation is due to leaching and erosion of the base and embankment, its strength is reduced leading to instability of the dam. The hydraulic conductivity of the core is strongly dependent on the core material and its compaction which directly determines the leaching rate [7]. Internal erosion is normally localised which makes it difficult to determine the leaching rate [6]. Traditionally to investigate internal erosion, visual inspection, pore-pressure measurements and measurement of leaching water volumes in dikes below the dam are used. It is therefore imperative for dam safety to be able to detect internal erosion by non-destructive methods at an early stage of development [6]. To be able to know the condition of dams due to safety reasons, dams need to be consistently monitored and inspected. Supervision and regular monitoring of the tailings impoundment with suitable methods are mostly needed to obtain high degree of dam safety. The technologies available for monitoring deformation of tailings dams can be grouped into static and dynamic deformation monitoring methods [8]. The static method includes photoelectric monitoring technology, mechanical deformation measurement, and high precision GPS deformation measurement [8]. The dynamic deformation monitoring methods are photogrammetry methods, 3D laser technique and real-time dynamic GPS methods. The selection of a method depends on the nature of dam and the accuracy required for the monitoring [8]. All these monitoring methods have different precision and adaptability.

To continue to ensure safety and predict the likelihood of tailings dam embankment collapse, there is the need for further studies using artificial intelligence techniques such as fractals to analyse the stability of tailings dams' embankment.

Mathematically, fractal dimension of a function can be expressed in different ways and assigned different sets of regularity measurements. Notwithstanding, mostly fractal evolution of α from f computed as against a particular quantity $\eta_{f(\alpha)}$ is dependent on the scale or resolution transformation of $f_\alpha$ of f. In this case, the fractal formalism indicates $\eta_{f(\alpha)}$ behaving as a power law with respect to the analysis scale α, and that the regularity strength has a relationship to the power law exponent.

Fractals define a set for which the Hausdorff-Besicovich dimension exceeding the topological dimension (e.g. 0 for

Yakubu I. is with the Department of Geomatic Engineering, University of Mines and Technology (UMaT), Tarkwa, Ghana (corresponding author, phone: +233 242957741; e-mail: yabsgm@gmail.com/ yissaka@umat.edu.gh).

Ziggah Y. Y. is with the Department of Geomatic Engineering, University of Mines and Technology (UMaT), Tarkwa, Ghana (e-mail: yyziggah@umat.edu.gh).

Yeboah C. is a national Service Personnel at Department of Geomatic Engineering, University of Mines and Technology (UMaT), Tarkwa, Ghana (e-mail: klemgee21@gmail.com).

points; 1 for lines; 2 for areas) [10]; in this case, D is usually designated as the fractal dimension (D = 2-H). H represents the Hurst Parameter. Fractal dimension indicates how compactly a phenomenon occupies the space in which it is located. Fractals establish a limit. It models complex physical processes and dynamic system [10]. The Hurst parameter gives a degree for long term memory and fractality of a time series [11]. Calculation of the Hurst parameter is achieved using rescaled range analysis, aggregated variable method, absolute moment's method etc. In this paper, the rescaled range analysis was considered.

A research conducted by [12] used fractal theory approach to analyse the landslide displacement in Wanzhou District in China. The fractal theory was valuable in appreciating the deformation history of different parts of the landslide. In this study, fractal theory was applied to evaluate the deformation of tailings dam embankment periodic surveyed data in a mine. The time domain of rescaled range analysis was chosen for the determination of the Hurst parameter. The evaluation of the Hurst parameter and the fractal dimension of tailings dam embankment based on the surveyed data established the stability of the tailings dam used in the area.

## II. Study Area

The study area (Fig. 1) is positioned at the mid-southern part of the Western Region of the Republic of Ghana [13] with geographic coordinates between longitude 2° 10′ 00″ E - 1° 45′ 00″ W and latitude 5º 25′ 00″ N - 4º 30′00″ S with an average topographic height of about 78 m above Mean Sea Level (MSL) [14]. Geographically, the topography is generally undulating with steep slopes parallel to each other and to the strike of the rocks in the North-South direction [15]. Currently, three large scale mining companies are operating in the area, namely; Goldfields Ghana Limited-Tarkwa Mine, AngloGold Ashanti-Iduapriem Mine and Ghana Manganese Company Limited-Nsuta. A host of small-scale mining groups are also scattered within the area. The activities of these mines have contributed to the socio-economic development of the area [16], [17].

In this study, a total of 650 secondary data (3D coordinates) of weekly monitored prisms over a one-year period was used. The dataset was collected on fixed prisms at faces of the tailing dam embankment of a mining company in the study area. The data were examined and outliers were filtered by using Kalman filtering technique.

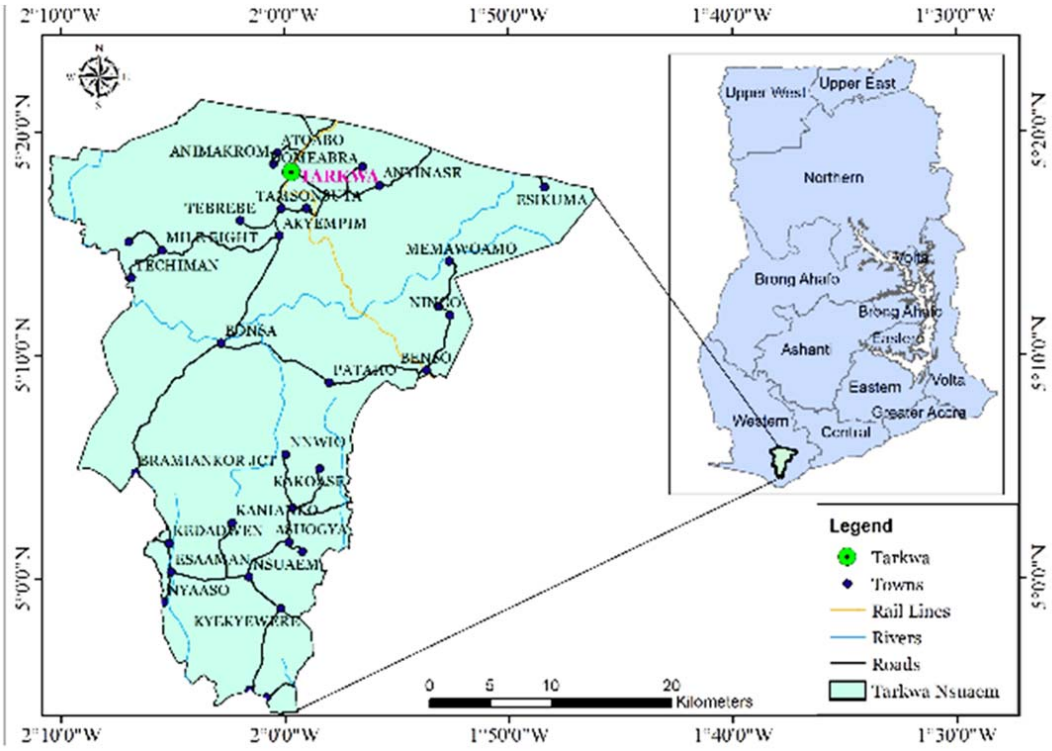


Fig. 1 Study Area

## III. Methods and Data

### A. Hurst Parameter and Rescale Range Analysis

Different exponent estimations can be used for the determination of the Hurst parameter. Amongst them are rescale range analysis estimation method, absolute moment estimation method, wavelet analysis method etc. The rescale range analysis estimation for the determination of the Hurst parameter was used in this paper.

The inception of rescale range analysis was by Hurst whilst working as a water Engineer in Egypt [18]. He then applied it to financial time series [19], [20]. It has been extensively used in studying persistence and long-term dependence in natural

time series. Reference [21] used rescaled range analysis to estimate the needed long-term storage for the Aswan high dam reservoir in Egypt. Previously, rescaled range analysis in conjunction with other more advanced methods have been extensively applied for the evaluation and modelling of persistence and long-term memory in real-world data in a variety of fields [22]. Amongst them are hydrology and water resources [23]-[25], geophysical records [26], [27] economics [28]-[30].

The rescale range analysis (R/S) is to help analyse the range which is taken as a measure of dissipation of the series to follow a scaling law [31]. If a process is random, the measure of dissipation scales with respect to the square-root law so that a power in the scaling law is equal to 0.5. Such value is connected to Hurst exponent of 0.5.

In this process, the returns of the time series of length T and then dividing them into N adjacent sub-periods of length ν while Nν=T [31]. Each sub-period is labeled as $I_n$ with n= 1, 2,… N. Additionally; each element in $I_n$ is labeled $r_{k,n}$ with k=1, 2, ..ν. Each sub-period calculates an average value and builds new series of accumulated deviations from the arithmetic mean values (a profile). This is then followed by the calculation of the range, which is the difference between a maximum and a minimum value of the profile $X_{k,n}$, and standard deviation of the original return series for each sub-period $I_n$. Each range $R_{In}$ is standardized by the corresponding standard deviation $S_{In}$ and forms a rescale range as

$$(R/S)_{In} = R_{In}/S_{In} \quad (1)$$

This process is then repeated for each sub-internal of length ν to obtain an average rescaled ranges $(R/S)_\nu$ for each sub-internal of length ν. The length ν is increased and the whole process is started over. The length ν equal to the exponent of a set integer value is used. Thus, a bias b, a minimum power pmin and a maximum power pmax so that $\nu = b^{pmin}, b^{pmin+1}, \ldots, b^{pmax} \leq T$ are set [32].

Rescaled range then scales as;

$$(R/S)_\nu \sim C_\nu^H \quad (2)$$

where C is a finite constant independent of ν [33], [34]. A linear relationship in double-logarithmic scale shows an exponent scaling [32]. To bring the scaling law to bare, an ordinary least squares regression on logarithms of each side of is used (2). Logarithm with basis equal to b is suggested. Thus,

$$\log_b (R/S)_\nu \sim \log_b{}^c + H\log_b{}^\nu \quad (3)$$

where H is the exponent.

The Hurst parameter is then determined using rescaled statistical (R/S) range analysis [18]. This method was employed in this study. The Hurst parameter (*H*) represents a statistical measure used to classify time series. The values of the Hurst parameter range between 0 and 1 [18]. The rescaled statistical estimator of *H* is given as:

$$E\left[\frac{R(\tau)}{S(\tau)}\right] = Cn^H \quad (4)$$

where $R(\tau)$ = amplitude range over a time window, τ, scaled to the standard deviation, $S(\tau)$ of the range.

$$R(\tau) = max\left(X\ (t,\tau)\ \right) - min\left(X\ (t,\tau)\right) \text{ and}$$

$$s(\tau) = \sqrt{\frac{1}{\tau}\sum_{t=1}^{\tau}(\xi(t) - (\xi)_\tau)^2} \quad (5)$$

where

$$X\ (t,\tau) = \sum_{u=1}^{t}\xi(u) - (\xi)_\tau \quad (6)$$

and

$$(\xi)_\tau = \frac{1}{\tau}\sum_{u=1}^{r}\xi(t) \quad (7)$$

The R/S for a given τ is $R/S(\tau) = \frac{R(\tau)}{S(\tau)}$ and H is the regression slope of log τ against log R/S(τ). In practice, in classical R/S analysis, *H* can be calculated using the slope of log/log plot of *t* (R / S) versus *t*. The H values were computed by scripting with MATLAB R2014a software using the rescaled range methodology and run against the calculated rate of movement of the original data. The *H* values computed were then used to derive the Fractal dimension of the dataset using the formula $D = 2 - H$ ,

*B Fractal Dimension*

A fractal object is made-up of scaled replicas of itself, it has an unlimited length and it is infinitely complex when the scale decreases. In this case, the object is self-similar at a variety of scales [35]. The fractal dimension, also known as the similarity dimension (D), shows basic characteristics of a fractal object and depicts the correlation between the apparent length and measurement scale [11]. Generally, fractal geometry has a shape characterised by distortions that cannot be explained by Euclidean structures. For ordinary Euclidean shapes, the *D* value of points is 0; line is 1; and area is 2. *D* is always an integer. But to measure the characteristic size of a fractal object by linear scaling, usually the results of *D* are not an integer and exceed the Euclidean dimension [36]. The framework on the evaluation of the fractal dimension is illustrated in Fig. 2.

The determination of *H* and *D* was based on the dataset obtained from the calculation of the rate of movement of the tailings dam embankment. The rate of movement was also computed from the monitored prism dataset from the walls of the tailings dam embankment. The rate of movement of each monitoring prism was used with the Rescaled Range estimator time domain to calculate for the Hurst parameter by coding using MATLABR2014a software.

## IV. Results and Discussion

Tables I and II show the results for the Hurst parameter and

Fractal dimension respectively.

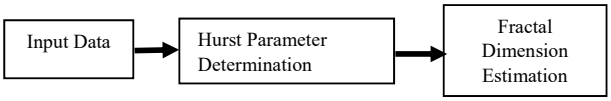


Fig. 2 Flowchart of Fractal Theory

TABLE I
ESTIMATED HURST PARAMETER

| Prism Name | Hurst Parameter (m) |
|---|---|
| MB 1 | $1.1570 \times 10^{-4}$ |
| MB 2 | $1.3699 \times 10^{-3}$ |
| MB 3 | $9.0940 \times 10^{-4}$ |
| MB 4 | $7.8070 \times 10^{-4}$ |
| MB 5 | $2.5880 \times 10^{-4}$ |
| MB 6 | $8.4440 \times 10^{-4}$ |
| MB 7 | $2.1920 \times 10^{-4}$ |
| MB 8 | $1.5023 \times 10^{-3}$ |
| MB 9 | $1.8641 \times 10^{-3}$ |
| MB 10 | $5.2210 \times 10^{-4}$ |
| MB 11 | $1.0013 \times 10^{-3}$ |
| MB 12 | $1.3940 \times 10^{-3}$ |
| MB 13 | $8.5040 \times 10^{-4}$ |
| MB 15 | $1.0638 \times 10^{-3}$ |
| MB 16 | $1.0324 \times 10^{-3}$ |

In [18], a smaller Hurst parameter gives a larger fractal dimension and a larger Hurst parameter gives a smaller fractal dimension. Comparatively, from the result in Tables I and II there was lesser deformation process occurring at prism MB 9 because of a smaller fractal dimension and hence making that particular prism point more stable and a higher deformation process at MB 1 due to a larger fractal dimension hence making that particular prism less stable.

Since the goal was to get a value range of 0 to 1 m from [18] with respect to the Hurst parameter, the results in Table I and II were within the threshold and are all stable. Also, the results approaching zero shows that, the fractal object was a point.

TABLE II
ESTIMATED FRACTAL DIMENSION

| Prism Name | Fractal Dimension (m) |
|---|---|
| MB 1 | $1.8843 \times 10^{-3}$ |
| MB 2 | $6.3010 \times 10^{-4}$ |
| MB 3 | $1.0906 \times 10^{-3}$ |
| MB 4 | $1.2193 \times 10^{-3}$ |
| MB 5 | $1.7412 \times 10^{-3}$ |
| MB 6 | $1.1556 \times 10^{-3}$ |
| MB 7 | $1.7808 \times 10^{-3}$ |
| MB 8 | $4.9770 \times 10^{-4}$ |
| MB 9 | $1.3590 \times 10^{-4}$ |
| MB10 | $1.4779 \times 10^{-3}$ |
| MB 11 | $9.9870 \times 10^{-4}$ |
| MB 12 | $6.0600 \times 10^{-4}$ |
| MB 13 | $1.1496 \times 10^{-3}$ |
| MB 15 | $9.3620 \times 10^{-4}$ |
| MB 16 | $9.6760 \times 10^{-4}$ |

## V. CONCLUSIONS

The following conclusions are made:

- The Hurst parameters of the monitored tailings dam embankment based on the surveyed dataset were determined, and are all within the threshold of $0 \leq H \leq 1\text{m}$;
- The fractal dimensions of the tailings dam embankment dataset were determined with values ranging from $1.359 \times 10^{-4}$ m to $1.8843 \times 10^{-3}$ m; and
- From the results of the Hurst parameter and fractal dimensions determined, the tailings dam embankment is very stable, since the results of all the monitored prisms were within the thresholds.

## REFERENCES

[1] Garland, R. (2011), "Acid mine drainage" the chemistry. pp. 50-52.
[2] Wehleekema, S. (2017), "Assessment of Iron Ore Mining Gangues in Itakpe for Secondary Recovery of Other Metal Values", Published MSc Thesis work, African University of Science and Technology, Abuja, Nigeria, 59pp.
[3] Thomas, A. (2016), "Effect of oxidative weathering on in vitro bioaccessibility of toxic substances in contaminated, mine tailings-borne dust", published MSc Thesis, The University of Arizona, Arizona, USA. pp.82.
[4] Davies, M. P. (2002), 'Tailings impoundment failures: are geotechnical engineers listening', Geotechnical News, vol. 20, no. 3, pp. 31–36.
[5] Wit T and Olivier G., (2018)," Imaging and monitoring tailings dam walls with ambient seismic noise" Paste 2018 – RJ Jewell and AB Fourie (eds) Australian Centre for Geomechanics, Perth, ISBN 978-0-9924810-8-7, pp. 455-463.
[6] Ganesh, M. (2006), "Monitoring of Tailings Dams with Geophysical Methods" (*Unpublished*) Thesis, Luleå University of Technology, pp. 93
[7] ICOLD, (1995), "Dam Failures Statistical" *Bulletin 99*, published by The International Commission on Large Dam together with UNEP, United Nations Environmental Program.
[8] Wei, L., and Chang, W. (2011), "GPS in the Tailings Dam Deformation Monitoring" *Procedia Engineering*, Vol. 26, pp.1648-1657.
[9] Flandrin, P, Rilling, G., and Goncalves, P. (2004), "Empirical Mode Decomposition as a Filter Bank", *IEEE Sig. Proc. Lett*. Vol. 11, No. 2, pp.112-114.
[10] Mandelbrot, B. B. (1977), "Fractals Form, Chance, and Dimension", W. H. Freeman and Company, San Francisco, USA, 1977. N-7491 Trodheim, Norway, pp.6; pp. 57-60.
[11] Mandelbrot, B.B, and Wallis, J. R. (1969), "Robustness of the rescaled range R/S in the measurements of noncyclic long-run statistical dependence, Water Resources, 5. pp. 967-988.
[12] Gui, L., Yin, K., and Glade, T. (2016), "Landslide displacement analysis based on fractal theory, in Wanzhou District, Three Gorges Reservoir", Faculty of Engineering, China University of Geosciences, Wuhan, China; Department of Geography and Regional Research, University of Vienna, Vienna, Austria. pp. 1707-1725.
[13] Asklunel, R., and Eldvall, B. (2005), "Contamination of Water Resources in Tarkwa Mining Area of Ghana", (*Unpublished*) MSc Thesis, Department of Engineering Geology, Royal Institute of Technology, LTh Ekosystemteknk, pp. 1-72.
[14] Boye, C. B., Peprah, M. S., and Kodie, N. K. (2018), "Geographic Assessment of Telecommunication Signals in a Mining Community: A Case Study of Tarkwa and Its Environs", Ghana Journal of Technology, Vol. 2, No. 2, pp. 41-49.
[15] Kortatsi, B. K. (2004), "Hydrochemistry of Groundwater in the Mining Area of Tarkwa-Prestea, Ghana", *(Unpublished*) PhD Thesis, University of Ghana, Legon-Accra, Ghana, pp. 1-45.
[16] Yakubu, I., Ziggah, Y. Y., and Peprah, M. S. (2018), "Adjustment of DGPS Data using Artificial Intelligence and Classical Least Square Techniques", *Journal of Geomatics*, Vol. 12, No. 1, pp. 13-20.\
[17] Peprah, M. S., Ziggah, Y. Y., and Yakubu, I. (2017), "Performance Evaluation of the Earth Gravitational Model (EGM2008) – A Case Study", *South African Journal of Geomatics*, Vol. 6, No. 1, pp. 47-72.
[18] Hurst, H. E. (1951), "Long term Storage of reservoirs: an Experimental

study", Transactions of the American Society of Civil Engineers, Vol. 116, pp. 770-799.
[19] Mandelbrot, B. and van Ness, J. (1968), "Fractional Brownian Motions, Fractional Noises and Applications" *SIAM Review*, Vol. 10, No. 4, pp. 422-437
[20] Mandelbrot, B. (1970), "Analysis of Long-Run Dependence in Economic: The R/S Technique" *Econometrica*, Vol. 39, pp. 107-108
[21] Hurst, H. E., R. P. Black, and Y. M. Simaika (1978), "The Nile Basin" Vol. 11. *Nile Control Department*, Ministry of Irrigation, Cairo, Egypt.
[22] Hamed, K. H. (2007), "Improved Finite-Sample Hurst Exponent Estimates Using Rescaled Range Analysis" *Water Resour. Res.,* 43, W04413, doi: 10.1029/2006WR005111
[23] Mandelbrot, B. B., and J. R. Wallis(1969a), "Robustness of the Rescaled Range R/S in the Measurement of Noncyclic Long Run Statistical Dependence ", *Water Resour*: *Res.,* Vol. 5, pp. 967-987
[24] Klemes, V., R. Srikanthan, and T. A. McMahon (1981), "Long-Memory Flow Models in Reservoir Analysis" What is their Practical Value?, *Water Resour. Res.,* Vol. 17, pp.737-751
[25] Hosking, J. R. M. (1984), "Modeling Persistence in Hydrological Time Series Using Fractional Differencing" *Water Resour. Res.,* Vol. 20, No. 12, pp. 1898-1908
[26] Mandelbrot, B. B., and J. R. Wallis (1969b), "Computer Experiments with Fractional Gaussian Noise" Part 1, 2, and 3, *Water Resour. Res.,* Vol 5, No. 1, pp.228-267
[27] Karner, O. (2002), "On Nonstationary and Antipersistency in Global Temperature Series", *J. Geophys. Res., 107(D20),* 4415, doi:10.1029/2001JD002024
[28] Lo, A. W. (1991), "Long–Term Memory in Stock Market Price", *Econometrica*, Vol. 59, No. 5, pp.1279-1313.
[29] Barkoulas, J., W. Labys, and J. Onochie (1999), "Long Memory in Commodity Future Prices", *Financ. Rev*., pp.117-132
[30] Giraitis, L., P. Kokoszka, R. Lepuis, and G. Teyssiere (2003), "Rescaled Variance and Related Tests for Long Memory in Volatility and Levels" *J. Econom.,* Vol. 112, pp. 265-294.
[31] Kristoufek, L. (2010), "Rescaled Range Analysis and Detrended Fluctuation Analysis: Finite Sample Properties Confidence Intervals" *AUCO Czech Economic,* Review 4, pp.236-250
[32] Weron, R. (2002), "Estimating Long-Range Dependence: Finite Sample Properties and Confidence Intervals", *Physica A*, Vol. 312, pp.285-299
[33] Taqqu, M., Teverosky, W. and Willinger , W. (1995), "Estimators for Long –Range Dependence: An Empirical Study" *Fractals*, Vol. 3, No. 4, pp.785-798
[34] Di Matteo, T. (2007), "Multi-Scaling in Finance "*Quantitative Finance*,Vol. 7, No. 1, pp.21-36
[35] Micallef A., Berndt C., Masson D. G., and Stow D. A.V. (2008), "Scale invariant characteristics of the Storegga Slide and implications for large-scale submarine mass movements", Mar Geol. Vol. 247, pp. 46-60.
[36] Sezer, E. (2010), "A computer program for fractal dimension (FRACEK) with application on type of mass movement characterization", Computer Geosciences, Vol.36, pp. 391-396.